haematologica
Journal of the Ferrata Storti Foundation

Potent synergy of DHODH and SREBP inhibition in acute myeloid leukemia via disruption of cholesterol and lipid metabolism

by Shanna M. Hogeling, Dominique Sternadt, Nikita La Rose, Marjan Geugien, Diego Pereira-Martins, Fiona A.J. van den Heuvel, Anna Kuchnio, E. Christine Pietsch, Ulrike Philippar, Gerwin Huls and Jan Jacob Schuringa

Received: March 28, 2025.
Accepted: December 1, 2025.

Citation: Shanna M. Hogeling, Dominique Sternadt, Nikita La Rose, Marjan Geugien, Diego Pereira-Martins, Fiona A.J. van den Heuvel, Anna Kuchnio, E. Christine Pietsch, Ulrike Philippar, Gerwin Huls and Jan Jacob Schuringa. Potent synergy of DHODH and SREBP inhibition in acute myeloid leukemia via disruption of cholesterol and lipid metabolism.
Haematologica. 2025 Dec 11. doi: 10.3324/haematol.2025.287918 [Epub ahead of print]

Potent synergy of DHODH and SREBP inhibition in acute myeloid leukemia via disruption of cholesterol and lipid metabolism

Shanna M. Hogeling[1], Dominique Sternadt[1], Nikita La Rose[1], Marjan Geugien[1], Diego Pereira-Martins[1], Fiona A.J. van den Heuvel[1], Anna Kuchnio[2], E. Christine Pietsch[3], Ulrike Philippar[2], Gerwin Huls[1] and Jan Jacob Schuringa[1*]

[1]Department of Hematology, University Medical Center Groningen, University of Groningen, Groningen, The Netherlands

[2]Discovery Oncology, Janssen Research & Development, Beerse, BE

[3]Discovery Oncology, Janssen Research & Development, Spring House, PA, USA

[*]correspondence:

Prof.dr. J.J. Schuringa, PhD

Department of Experimental Hematology

University Medical Center Groningen

Hanzeplein 1, PO Box 30.001, 9700 RB Groningen, The Netherlands

Phone: + 31503612354, Fax: +31503615960

E-mail: j.j.schuringa@umcg.nl

Running head: Synergistic DHODH/SREBP inhibition in AML

Funding

The authors disclose no conflicts of interest. This work was supported by a grant from the Dutch Cancer Foundation to JJS (11013), an EU EP PerMed grant MetaboTargetAML to JJS (ZonMW 11180102410004) and a PPP grant from Health Holland/TKI (LSHM200204)

Author contributions

S.M.H. and J.J.S. conceived and designed the study; S.M.H., D.S. N.L.R., M.G., D.P.M., F.A.J.H., and J.J.S. performed experiments, analyzed, and interpreted data, performed statistical analysis, and drafted the article; A.K., C.P., U.P. provided compounds; A.K., C.P., U.P. and G.H. interpreted data; G.H. provided patient samples and clinical data; S.M.H and J.J.S. wrote the paper which was reviewed by all authors. All authors gave final approval of the submitted manuscript.

Declaration of interests: The authors have no competing financial interests. A.K., C.P. and U.P. are current employees of Janssen Research & Development and may own stock/stock options in Johnson & Johnson.

Data sharing statement: All data is available in the manuscript and is also available upon request.

Abstract

Acute myeloid leukemia (AML) remains difficult to cure, in part related to strong genetic and functional heterogeneity between and within individual patients. Metabolic reprogramming is emerging as an important feature of AML cells, allowing to explore alternative treatment strategies. Here, we describe a novel DHODH inhibitor, JNJ-74856665, that showed strong efficacy in a subset of AML samples. In a multi-omics approach, by combining label-free quantitative proteome data with drug sensitivity data in bone marrow stromal cocultures in a large cohort of primary AML patient samples we identified that sensitivity to DHODH inhibition (DHODHi) is linked to cholesterol and lipid metabolism. DHODHi resulted in an accumulation of cholesterol, mitochondrial ROS and lipid peroxidation. LC-MS/MS-based lipidomics studies revealed that DHODHi resulted in a strong increase in polyunsaturated fatty acids (PUFAs) and triglycerides (TGs), which are the primary lipid species stored in lipid droplets (LDs). We hypothesized that this might be the consequence of increased ROS and lipid peroxidation levels, prompting the cell to detoxify such toxic lipid species by storing them in LDs. Indeed, we could observed a marked increase in LD formation upon DHODHi. The transcriptional regulator SREBF2, known to control cholesterol and lipid metabolism, was upregulated in DHODHi sensitive AMLs, and a strong synergy was observed between combination of both DHODHi and the SREBP inhibitor dipyridamole. Our data indicate that combined DHODH and SREBP inhibition is of interest to explore further as a therapeutic target option in AML.

Introduction

Acute myeloid leukemia (AML) is a heterogeneous disease, where a block in differentiation leads to the accumulation of immature myeloid blasts. Despite ongoing improvements in diagnosis and therapies, the treatment of AML remains challenging with the '3+7' chemotherapy backbone serving as the basis for current treatment. A promising addition to cancer therapy is the recent emergence of dihydroorotate dehydrogenase (DHODH) inhibition, which is the rate limiting step in the *de novo* pyrimidine synthesis pathway. As an important step in the pathway it converts dihydroorotate (DHO) to orotate, a substrate for uridine monophosphate (UMP) that can be further converted to other pyrimidine nucleotides needed in proliferating cells.[1] In AML, DHODH was identified as one of the main targets to overcome the block in differentiation.[2–4] Here, by integrating proteogenomic data with our *ex vivo* drug screening platform in primary AML patient samples we studied the effect of a novel DHODH inhibitor, JNJ-74856665.[5] By integration of this dataset, we aimed to gain insight into which AML subtypes benefit the most from DHODH inhibition (DHODHi) and explore synergistic drug combinations. We identified that sensitivity to DHODHi is linked to cholesterol and lipid metabolism, which could be targeted with dipyridamole, and combination treatment resulted in strong synergistic cell death as a consequence of ROS and lipid ROS accumulation, combined with impaired cholesterol metabolism and lipid detoxification.

Methods

Primary samples

AML blasts from peripheral blood or bone marrow from untreated patients and normal bone marrow (NBM) samples were obtained from healthy individuals at the University

Medical Center Groningen after informed consent and the protocol was approved by the Medical Ethical Committee, in accordance with the Declaration of Helsinki. Mononuclear cells (MNCs) were isolated via Lymphoprep^{TM} separation and cryopreserved. Next Generation Sequencing was performed to obtain mutation status of primary AML cells using the TruSight Myeloid Sequencing Panel (Illumina) or exome sequencing. Neonatal cord blood (CB) samples were obtained from healthy full-term pregnancies at the obstetrics departments at the Martini Hospital and University Medical Center Groningen

Cell culture

The AML cell lines THP1 (DSMZ: ACC-16) and HL60 (DSMZ: ACC-3) cells were cultured in RPMI 1640 with 10% FCS and 1% P/S. MS5 murine stromal cells (DSMZ: ACC-441) were cultured in alpha-MEM (Lonza) with 10% FCS and 1% P/S. All cell cultures were kept at 37°C and 5% CO_2. Inhibitor JNJ-74856665 was provided by Janssen Biologics BV for all DHODHi experiments. Diyridamole, Dilazep and Betulin were obtained from MedChemExpress (Monmouth Junction, USA)). Atorvastatin and Rosuvastatin were obtained from Axon Medchem (Groningen, NL).

DHODH inhibitor screen in primary AML samples

Cryopreserved MNCs of AML patients were co-cultured in Gartner's medium supplemented with G-CSF (Amgen), N-Plate (TPO)(Amgen) and IL-3 (Sandoz) (all 20 ng/mL) on MS5, which were confluent plated on 0.1% gelatin-coated 96 wells plates and pre-treated with Mitomycin C. 100.000 MNCs per well were plated per well, and after two days recovery cells were treated with DMSO or 0.3, 3.00, 30.0 and 300 nM JNJ-74856665 inhibitor for seven days. On day 7 cells were stained with

CD45-PECy7 (BioLegend; 304016), CD14-PE (BioLegend; 325606), CD11b-FITC (ImmunoTools; 21279113X2), and DAPI (ThermoScientific) in a 96 wells plate, and were incubated for 30 min at 4°C. Fluorescence measurements were taken using a MACSQuant® X Flow Cytometer (Miltenyi Biotec).

DHODH inhibitor screen in healthy samples

Healthy MNCs were isolated from NBM by a density gradient using Lymphoprep™ (STEMCELL™ Technologies). Stem cells were isolated using the CD34 Microbead Kit (Miltenyi). After 24h recovery in Stemline® II hematopoietic medium (Merck; #S0192) supplemented with 1% P/S, SCF, FLT3-L and N-plate (TPO)(Amgen)(all 100 ng/mL), $CD34^+$ NBM cells were treated with DMSO or 0.3, 3.00, 30.0 and 300 nM JNJ-74856665 inhibitor for seven days and co-cultured on MS5 in Gartner's medium supplemented with cytokines.

Flow cytometry data analysis inhibitor screen

All flow data was analysed using Flow Jo™ (BD BioSciences). Counts, percentages and Median Fluorescent Intensities were exported for further analysis. To calculate area under the curve (AUC) values $DAPI^-/CD45^{dim}$ (primary samples) or $DAPI^-$ (cell lines) counts were normalized to the DMSO control. Next, AUC was calculated using trapezoid rule integration computed by the trapz() function in the R package caTools. CD11b MFI values were normalized to DMSO control.

Inhibitor combination treatments

AML cell lines, primary AML patient cells and $CD34^+$ cord blood (CB) cells were treated with DMSO or 0.3, 3.00 and 30.0 nM JNJ-74856665 inhibitor for three days in

combination with Dipyridamole (DMSO or 1, 5 and 10 µM), Betulin (DMSO or 5, 10 and 20 µM), Dilazep (DMSO or 0.1, 1 and 10 µM), Atorvastatin (DMSO or 2, 10 and 20 µM) or Rosuvastatin (DMSO or 0.3, 3 and 30 µM). After three day incubation, cells were stained with Annexin-V APC, CD11b-FITC, CD14-PE and 7AAD for DHODH and Dipyridamole treated cells. The other combinations were stained with Annexin-V APC and DAPI. All stainings were done in a 96 well plate and incubated for 30 minutes at 4°C. Fluorescence measurements were taken using a MACSQuant® X Flow Cytometer (Miltenyi Biotec). Flow data was analyzed using Flow Jo™ (BD BioSciences) and ZIP scores were calculated using SynergyFinder 3.0 [6].

ROS, BODIPY cholesterol, neutral lipid and mitochondrial measurements

After treatment 100.000 cells were taken and washed twice with PBS. Next, cells were resuspended in medium containing ROS–DCF-DA (10 µM) (Merck; #35845), the mitochondrial superoxide probe MitoSOXTM (5 µM) (ThermoScientific; #M36008) or C11-BODIPY (lipid ROS) (Thermofisher #D3861) or cell were resuspended in PBS containing BODIPY-cholesterol (MedChemExpress; #HY-125746), BODIPY™ 493/503 (Invitrogen™ #D3922), Tetramethylrhodamine, Ethyl Ester, Perchlorate (TMRE) (Thermofisher #T669) or MitoTracker GreenTM (Thermofisher #M7514). Additionally, verapamil hydrochloride (12.5 µM) was added to all staining procedures to prevent efflux of the mitochondria related probes. Fluorescence measurements were taken using a MACSQuant® X Flow Cytometer (Miltenyi Biotec) or a NovoCyte Quanteon (Agilent). All flow data was analysed using Flow Jo™ (BD BioSciences). For each sample a minimum of 10000 events were acquired inside the viable gate.

Lipidomics

Sample preparation for LC-MS/MS

To each 75 µL cell suspension 200 µL methanol containing 1000x diluted EquiSPLASH internal standard (Avanti) was added and vortexed well. 625 µL MTBE (methyl tert-butyl ether) was added and incubated for 1 h on a shaker at 900 rpm. 100 µL water was added and incubated on a shaker at 900 rpm for 10 min. Extracts were centrifuged at 1000 x g for 10 min and the upper organic phase was collected in a separate tube. The lower phase was re-extracted with 250 µL solvent mixture (MTBE/methanol/water 10:3:2.5 v/v/v), and incubated on a shaker for 30 min at 900 rpm. Extracts were centrifuged at 1000 x g for 3 min and the upper organic phase was added to the organic phase of the first extraction. The combined organic phases were concentrated under a heated nitrogen stream (50 °C) and subsequently dried in a vacuum centrifuge at 30 ºC. Dried lipid pellets were dissolved in 25 µL CH3Cl/methanol/water 60:30:4.5 v/v/v and with 75 µL isopropanol/acetonitrile/water 2:1:1 v/v/v.

Results

Primary AML patient samples were analyzed for mutation status (Illumina Trusight sequencing, n=26, Supplementary Table 1), full label-free quantitative proteome (LC-MS/MS, n=17[7]) and for DHODH inhibitor (DHODHi) sensitivity on MS5 bone marrow stromal cells (n=26). The inhibitor was tested at a range of 0.3 – 300 nM and after seven days the effects on proliferation, viability and differentiation were determined by flow cytometry (Figure 1A, Supplementary Figure 1A). *Ex vivo* culturing of primary AML samples can be challenging and therefore stromal cocultures were used given their superior long-term support of primary AML patient samples compared to liquid culture conditions[8–11], and only samples were included where the viability could be

maintained throughout the experiments (Supplementary Figure 1B-C). Area under the curve (AUC) values were determined based on viable $DAPI^-/CD45^{dim}$ blast counts, which revealed a strong but heterogenous response to the inhibitor (Figure 1B-C). An induction of differentiation based on increased CD11b expression was also noted in some (n=8; AML28, 32, 31, 30, 8, 29, 14, and 6) but not all AML patient samples. Not all samples in which proliferation and viability were most strongly inhibited responded by inducing differentiation, suggesting that these processes are not directly linked (Figure 1B). One of the functions of DHODH entails the rate limiting step in *de novo* pyrimidine synthesis, which is upregulated in proliferating cells as response to the increased demand of nucleotides needed for DNA synthesis. Indeed, while we observed a trend towards inverse correlations between the proliferation rate of unperturbed cells and AUC values this did not reach significance (Supplementary Figure 1D), suggesting that other functions downstream of DHODH might also play an important role. No significant correlations were observed between mutation status and response to DHODHi, but larger cohort sizes may be needed to identify such associations (Supplementary Figure 1E). At lower concentrations, healthy $CD34^+$ cells derived from normal bone marrow were less sensitive compared to AML samples (Figure 1D). To gain a better understanding of the protein expression programs that underlie DHODH inhibitor sensitivity we analyzed the full proteome of primary AML patients included in the drug screen (n=17).[12] We calculated Pearson correlation coefficients between the quantitative proteome dataset and AUC values of the DHODHi (Figure 2A). Subsequently, the ranked Pearson correlation coefficient list was used for gene set enrichment analysis (GSEA), which showed that DHODHi sensitive AML samples were enriched for signatures related to ‘cholesterol metabolism’, ‘biosynthesis of unsaturated fatty

acids', 'glutathione conjugation', 'membrane lipid biosynthetic process', 'PPAR signalling pathway' and 'cholesterol biosynthesis'. Indeed, sterol regulatory binding transcription factor 2 (SREBF2), which controls expression of genes related to cholesterol synthesis and genes associated with lipid synthesis and detoxification such as SCD1[13–16] and DGAT1/2[17,18], was upregulated in AML samples with high sensitivity to DHODHi (Figure 2A). These data suggest that AML samples with an increased cholesterol metabolism and/or lipid metabolism would be most dependent on DHODH activity. Reversely, insensitive AML samples were enriched for signatures like 'MYC targets', 'KEGG spliceosome' and 'KEGG Ribosome' (Figure 2B-C).

To further explore potential downstream mechanisms that mediate DHODHi sensitivity, we treated AML cell lines HL60 and THP1 with the inhibitor. Proliferation was impaired in both cell lines, albeit that HL60 cells were slightly more sensitive compared to THP1 (Supplementary Figure 1F-G). This was accompanied by an increase in apoptosis as determined by Annexin V staining as well as an induction of differentiation (Supplementary Figure 1F-G). We also observed a significant increase in the amount of total cholesterol accumulation in the cells upon DHODHi, possibly as a consequence of reduced proliferation (Figure 3A). In addition, DHODH is suggested to regulate reactive oxygen species (ROS) production and ferroptosis.[19] Thus, we wondered if DHODHi would change ROS levels in HL60 and THP1 cells. Mitochondrial superoxide levels (MitoSox) and lipid ROS (BODIPY-C11) were significantly increased in both cell lines after treatment with DHODHi (Figure 3B). Cytoplasmic ROS levels were only significantly increased in HL60 cells upon DHODHi. As expected, mitochondrial activity as determined by TMRE was

decreased upon DHODHi, as a consequence of impairing the electron transport chain (ETC), while the total of mitochondria remained unchanged (Figure 3B).

We did wonder whether similar or different mechanisms would underly sensitivity in these two AML models, as we previously showed that the metabolism of these cell lines is quite different, with HL60 being more glycolytic and THP1 being more oxidative phosphorylation (OXPHOS)-driven.[20,21] Indeed, THP1 cells displayed higher basal levels of mitochondrial and cytoplasmic ROS, while total lipid ROS levels were comparable (Figure 3C). From these data we hypothesized that the effects of DHODHi in THP1 cells might derive primarily from inhibition of the ETC as compared to HL60 cells. We then performed single sample GSEA analyses on the top eight DHODHi-sensitive AML samples focussing on gene sets associated with metabolism. Although all sensitive samples had cholesterol and lipid metabolism as commonly enriched terms (Figure 2A-C), differences existed as well (Supplementary Figure 2). Specifically, some of the DHODHi sensitive cells were more enriched for processes related to mitochondrial respiration and ETC, while others were more enriched for glycolysis. Additionally, a subset of samples showed specific enrichment for lipid droplet formation. Together, these data indicate that distinct processes downstream of DHODH might underly sensitivity in individual AMLs.

To explore this further, we performed LC-MS/MS-based lipidomics studies in both AML models, in the absence or presence of DHODHi. These data revealed a profound impact of DHODHi on the lipidome (Figure 4, Supplementary Figure 3), with most notably a strong increase in triglycerides (TGs). In THP1 cells, but not HL60 cells, a strong decrease in acylcarnitines (CAR) was observed upon DHODHi (Supplementary Figure 3A-B), whereby baseline CAR levels were much higher in THP1 (Supplementary Figure 3C-D), again in line with the notion that THP1 cells are

more OXPHOS-driven[21], in part via fatty acid oxidation (FAO), which was impaired by inhibiting the ETC upon treatment with DHODH inhibitors. A significant increase in cholesterol esters (CEs) was also observed in HL60 (Figure 4A-B), but in THP1 cells where levels went down, while THP1 did display higher basal levels compared to HL60 (Supplementary Figure 3B, D). A remarkable shift in the degree of lipid chain unsaturation was observed, with an increase in polyunsaturated fatty acids (PUFAs) upon DHODHi (Figure 4C, Supplementary Figure 3E). When ROS levels increase, PUFAs run the risk of becoming peroxidated resulting in ferroptosis.[22] TGs are the primary lipid species stored in lipid droplets (LDs), [23,24] and we therefore hypothesized that the increase in TGs upon DHODHi could be a consequence of increased ROS and lipid peroxidation levels, promoting detoxification by storing toxic lipid species in LDs. Indeed, we observed a significant increase in TG PUFAs (Figure 4D, Supplementary Figure 3F) as well as the formation of LDs upon DHODHi (Figure 4E, Supplementary Figure 3G).

One of the key regulatory transcription factor families involved in cholesterol and lipid metabolism is the family of sterol regulatory element-binding proteins (SREBPs), and as outlined above we noted a significant upregulation of SREBF2 in cells that are most sensitive to DHODHi (Figure 2A). It has been shown that the phosphodiesterase inhibitor dipyridamole, an FDA-approved antiplatelet agent,[25] can inhibit the activation of SREBPs and their target genes.[26] Therefore, we wanted to explore whether treatment with dipyridamole would enhance the inhibitory effect of DHODHi. Single treatment experiments indicated that HL60 cells are slightly sensitive, but THP1 cells are not sensitive to dipyridamole alone at low concentrations (Figure 5A-B). When treating THP1 cells with higher concentrations of dipyridamole up to 40 μM, we did see a significant effect on proliferation

(Supplementary Figure 4A). Baseline cholesterol levels were also higher in THP1 compared to HL60 (Figure 5C and Supplementary Figure 3C-D), and only in HL60 a reduction in cholesterol levels could be achieved upon dipyridamole treatment alone at low concentrations (Figure 5C). In addition, the amount of cholesterol in THP1 cells was decreased upon treatment with higher concentrations of dipyridamole (Supplementary Figure 4B). In line, we also noticed higher mRNA expression levels of genes involved in the cholesterol metabolism pathway in THP1 cells when compared to HL60 (Supplementary Figure 4C), which was confirmed by Q-RT-PCR for *DHCR7* and *HMGCS1* (Figure 5D). Treatment with dipyridamole resulted in reduced expression of DHCR7 and HMGCS1, albeit that this occurred within 6 hours in HL60 and only after 96 hours in THP1 (Figure 5E).

Combination treatment with both DHODHi and dipyridamole showed strong synergy in both cell lines with ZIP scores of 27.6 and 32.5 for the HL60- and THP1-treated cells, respectively, as determined by SynergyFinder[27] where a ZIP score > 10 was considered as synergistic (Figure 5A-B). Combination treatment resulted in high levels of apoptosis, and induction of differentiation was also observed (Figure 5F). Similar results were obtained in primary AML patient samples. AML3, AML6, AML14 and AML27 were co-cultured on MS5 and were treated with single agents or combinations. There was no effect on proliferation with dipyridamole as single treatment in 2 of the 4 primary AML samples, AML3 and AML6, while slight reductions in proliferation were seen in AML14 and AML27 (Supplementary Figure 4D). But similar to our observations in cell lines, the combination treatment of DHODHi and dipyridamole was strongly synergistic in all cases with ZIP scores of 35.5, 29.1, 27.0, and 11.1, respectively (Supplementary Figure 4D). After these four initial samples an additional ten patient samples were analysed in combination

treatment studies. Again, combination treatment resulted in strongly reduced cell counts and an induction of differentiation (Supplementary Figure 4E). Normal $CD34^+$ cells were less sensitive to combination treatment of DHODH and SREBP inhibition, particularly at lower DHODH inhibitor concentrations (Supplementary Figure 5A), without consistent induction of differentiation (Supplementary Figure 5B-C). Previous studies have also discussed the combination treatment of DHODH and dipyridamole, which was positioned as a known inhibitor of the nucleoside/nucleotide transport channels hENT1/2 (SLC29A1-A2).[28] To address this further we evaluated the efficacy of DHODHi in combination with dilazep, an ENT1 inhibitor. While combination treatment was additive in HL60 cells, it was synergistic in THP1 and two primary AML samples, albeit that ZIP scores were not as high as with the DHODH/dipyridamole combination (Supplementary Figure 6A-B). Clearly, the salvage pathway might also play a role downstream of SREBP, albeit it to a lesser extent in HL60 cells, possibly due to their glycolytic-driven metabolism. To further address the potential link with cholesterol metabolism we used the specific inhibitors rosuvastatin and atorvastatin, which target HMG-CoA reductase, crucial for cholesterol synthesis. Combination treatment of these inhibitors together with DHODHi resulted in additive to synergistic effects (Supplementary Figure 6C-F), but again with lower ZIP scores compared to the DHODH/dipyridamole combination. Interestingly, inhibition of cholesterol metabolism in combination with DHODHi displayed stronger effects in HL60 compared to THP1, again highlighting the heterogeneity in metabolic vulnerabilities across different AML subtypes.

Discussion

By combining label-free quantitative proteome data with drug sensitivity screens in primary AML patient samples co-cultured on bone marrow stroma, we show here that sensitivity to the DHODH inhibitor JNJ-74856665 is linked to cholesterol and lipid metabolism. The transcriptional regulator SREBF2 was upregulated in DHODHi sensitive AMLs, and a strong synergy was observed between DHODH inhibition and the SREBP inhibitor dipyridamole. Our data indicate that several pathways downstream of dipyridamole might account for the synergistic actions together with DHODHi, including its control over cholesterol metabolism, over nucleoside/nucleotide import, and over lipid detoxification via lipid droplet formation.

The DHODH enzyme exerts several functions in the cell. It controls pyrimidine nucleotide synthesis by catalyzing the oxidation of dihydroorotate to orotate, the base precursor of pyrimidines.[29] During this reaction, the electron acceptor ubiquinone is reduced to ubiquinol, thereby providing electrons from the ETC complex I/II to complex III and thereby maintaining mitochondrial OXPHOS and ATP production. Furthermore, it has been shown that DHODH controls protein O-linked N-acetylglycosylation via the generation of UDP-GlcNAc.[3] Restored differentiation in AML upon DHODHi was attributed, at least in part, to depletion of UDP-GlcNAc leading to decreased O-linked N-acetylglycosylation.[3] Indeed, we observe strong heterogeneity in responses toward inhibition of DHODH across a panel of primary AML patient samples. While some samples responded strongly in terms of loss of proliferation and viability, others were much less sensitive. Within our cohort of 26 samples, sensitivity was not associated with a specific genetic subtype of AML. We initially hypothesized that sensitivity might be linked to proliferation, and while we indeed observed a trend between sensitivity and relative growth levels during our

culture periods, this did not reach significance, leaving open the possibility that other characteristics would underly DHODHi sensitivity.

We and others have shown that metabolic programs can differ considerably between AML subtypes.[11,20,21,30–34] By linking DHODHi sensitivity to protein expression programs, we identified that the most sensitive AMLs were characterized by high cholesterol and lipid metabolism. The transcription factor family of sterol regulatory element-binding proteins (SREBPs) controls expression of enzymes involved in cholesterol and lipid metabolism[17], including HMGCS1, HMGCR1, SQLE, DHCR7/24 as well as SCD1 which converts saturated fatty acids into mono-unsaturated acids (MUFAs) and DGAT1/2 which is essential for lipid droplet formation, thereby playing an important role in the detoxification of lipids. Based on these initial findings, and since SREBF2 was among the upregulated proteins in DHODHi-sensitive AMLs, we tested efficacy of dipyridamole in combination with inhibition of DHODH, and uncovered potent synergistic effects. We wondered whether the underlying mechanisms explaining these synergistic effects would be similar across different AML subtypes, and therefore performed extensive lipidomics studies and utilized more specific inhibitors to inhibit cholesterol metabolism or the nucleotide salvage pathway by inhibiting ENT importers. For this, we used two AML model systems, the glycolytic cell line HL60 and the OXHPOS-driven cell line THP1. In both cell lines inhibition of DHODH resulted in increased levels of PUFAs as well as increased levels of TGs. The latter is indicative for lipid droplet formation, as we have also observed that inhibition of DGAT1 results in strong reductions of TGs (Sternadt et al, accepted for publication in Blood Advances; data not shown). These data would suggest that the increase in ROS and lipid ROS levels as a consequence of DHODHi would drive a cellular response by detoxifying these toxic lipid species in lipid

droplets, which would be counteracted by SREBP inhibition. These data are in line with a recent publication where DHODHi in $CD8^+$ T cells also resulted in increased ferroptosis and PUFA accumulation.[35] While mitochondrial ROS was increased upon DHODHi in both HL60 and THP1 cells, cytoplasmic ROS levels were only increased in HL60 cells, even though lipid ROS, lipid droplet, and TG levels were increased in both models. The reason behind this remains unclear, but our observations suggest that the timing of measuring ROS and lipid ROS can be critically important, whereby at later timepoints all ROS species may have already been incorporated into lipids. We speculate that this might have been the case in our THP1 measurements, but further studies are clearly required.

While part of the phenotypes of the DHODHi/dipyridamole combination could be phenocopied by combining DHODHi with inhibitors against cholesterol metabolism or the pyrimidine salvage pathway, ZIP scores were never as high as those seen with the DHODHi/dipyridamole combination. Furthermore, slight differences between AML models were observed, whereby THP1 was more sensitive to the combination with ENT inhibitors while HL60 cells were more sensitive to combined inhibition of cholesterol metabolism. These observations highlight the heterogeneity across the AML landscape but also further underscore the potential of SREBP inhibition together DHODHi as several important pathways can be affected.

The impact of DHODHi and its combination with dipyridamole on myeloid differentiation was also noted in a subset but not all AML cases, in line with data by Branstrom *et al.*[36] where two out of five tested primary AML patient samples with DHODH inhibitor Emvodostat showed differentiation. There was no clear correlation between the impact of DHODHi on proliferation and differentiation. While differentiation was affected in some cases, this was not consistently observed among

all strong responders in terms of proliferation and apoptosis. The number of samples in which differentiation was induced was relatively small in our cohort which did not allow further functional studies to the mechanisms that might underly these observations.

A limitation of the current study is the lack of *in vivo* models and future studies will be required to evaluate efficacy of the DHODHi/dipyridamole combination *in vivo* in patient-derived xenograft models. Clinical trials with DHODH inhibitors (e.g. JBZ-001; BAY2402234) showed acceptable tolerability, albeit that some of these trials were stopped prematurely due to insufficient efficacy, pinpointing the need for combination treatments. Additionally, dipyridamole is widely used in the clinic as a well-tolerated antiplatelet medicine. It is typically used at 75-100 mg four times daily, reaching plasma concentrations of 0.5-1.9 ug/ml, which is in the low nM range as also used in our experiments. Whether a therapeutic window also exists in primary patients remains to be determined in follow-up studies, but our data indicate that combined DHODH and SREBP inhibition is of interest to explore further.

References

1. Boukalova S, Hubackova S, Milosevic M, Ezrova Z, Neuzil J, Rohlena J. Dihydroorotate dehydrogenase in oxidative phosphorylation and cancer. Biochim Biophys Acta Mol Basis Dis. 2020;1866(6):165759.
2. Christian S, Merz C, Evans L, et al. The novel dihydroorotate dehydrogenase (DHODH) inhibitor BAY 2402234 triggers differentiation and is effective in the treatment of myeloid malignancies. Leukemia. 2019;33(10):2403-2415.
3. Sykes DB, Kfoury YS, Mercier FE, et al. Inhibition of Dihydroorotate Dehydrogenase Overcomes Differentiation Blockade in Acute Myeloid Leukemia. Cell. 2016;167(1):171-186.e15.
4. Zhou J, Yiying Quah J, Ng Y, et al. ASLAN003, a potent dihydroorotate dehydrogenase inhibitor for differentiation of acute myeloid leukemia. Haematologica. 2020;105(9):2286-2297.
5. Cisar JS, Pietsch C, DeRatt LG, et al. N-Heterocyclic 3-Pyridyl Carboxamide Inhibitors of DHODH for the Treatment of Acute Myelogenous Leukemia. J Med Chem. 2022;65(16):11241-11256.
6. Ianevski A, Giri AK, Aittokallio T. SynergyFinder 3.0: an interactive analysis and consensus interpretation of multi-drug synergies across multiple samples. Nucleic Acids Res. 2022;50(W1):W739-W743.
7. Hogeling SM, Lê DM, La Rose N, et al. Bleximenib, the novel menin-KMT2A inhibitor JNJ-75276617, impairs long-term proliferation and immune evasion in acute myeloid leukemia. Haematologica. 2025;110(6):1278-1291.
8. Sontakke P, Carretta M, Capala M, Schepers H, Schuringa JJ. Ex vivo assays to study self-renewal, long-term expansion, and leukemic transformation of genetically modified human hematopoietic and patient-derived leukemic stem cells. Methods Mol Biol. 2014;1185:195-210.
9. Schuringa JJ, Schepers H. Ex vivo assays to study self-renewal and long-term expansion of genetically modified primary human acute myeloid leukemia stem cells. Methods Mol Biol. 2009;538:287-300.
10. van Gosliga D, Schepers H, Rizo A, van der Kolk D, Vellenga E, Schuringa JJ. Establishing long-term cultures with self-renewing acute myeloid leukemia stem/progenitor cells. Exp Hematol. 2007;35(10):1538-49.
11. de Boer B, Prick J, Pruis MG, et al. Prospective Isolation and Characterization of Genetically and Functionally Distinct AML Subclones. Cancer Cell. 2018;34(4):674-689.e8.
12. Hogeling SM, Lê DM, La Rose N, et al. Bleximenib, the novel menin-KMT2A inhibitor JNJ-75276617, impairs long-term proliferation and immune evasion in acute myeloid leukemia. Haematologica. 2025;110(6):1278-1291.

13. Vergnes L, Chin RG, de Aguiar Vallim T, et al. SREBP-2-deficient and hypomorphic mice reveal roles for SREBP-2 in embryonic development and SREBP-1c expression. J Lipid Res. 2016;57(3):410-421.

14. Wu Y, Song W, Su M, He J, Hu R, Zhao Y. The Role of Cholesterol Metabolism and Its Regulation in Tumor Development. Cancer Med. 2025;14(7):e70783.

15. Li N, Li X, Ding Y, et al. SREBP Regulation of Lipid Metabolism in Liver Disease, and Therapeutic Strategies. Biomedicines. 2023;11(12):3280.

16. Shimano H. Sterol regulatory element-binding proteins (SREBPs): transcriptional regulators of lipid synthetic genes. Prog Lipid Res. 2001;40(6):439-452.

17. Horton JD, Goldstein JL, Brown MS. SREBPs: activators of the complete program of cholesterol and fatty acid synthesis in the liver. J Clin Invest. 2002;109(9):1125-1131.

18. Xu HF, Luo J, Zhao WS, et al. Overexpression of SREBP1 (sterol regulatory element binding protein 1) promotes de novo fatty acid synthesis and triacylglycerol accumulation in goat mammary epithelial cells. J Dairy Sci. 2016;99(1):783-795.

19. Mao C, Liu X, Zhang Y, et al. DHODH-mediated ferroptosis defence is a targetable vulnerability in cancer. Nature. 2021;593(7860):586-590.

20. Erdem A, Marin S, Pereira-Martins DA, et al. Inhibition of the succinyl dehydrogenase complex in acute myeloid leukemia leads to a lactate-fuelled respiratory metabolic vulnerability. Nat Commun. 2022;13(1):2013.

21. Erdem A, Marin S, Pereira-Martins DA, et al. The Glycolytic Gatekeeper PDK1 defines different metabolic states between genetically distinct subtypes of human acute myeloid leukemia. Nat Commun. 2022;13(1):1105.

22. Stockwell BR, Friedmann Angeli JP, Bayir H, et al. Ferroptosis: A Regulated Cell Death Nexus Linking Metabolism, Redox Biology, and Disease. Cell. 2017;171(2):273-285.

23. Thiam AR, Farese RV, Walther TC. The biophysics and cell biology of lipid droplets. Nat Rev Mol Cell Biol. 2013;14(12):775-786.

24. Walther TC, Farese RV. Lipid droplets and cellular lipid metabolism. Annu Rev Biochem. 2012;81:687-714.

25. Sacco RL, Adams R, Albers G, et al. Guidelines for prevention of stroke in patients with ischemic stroke or transient ischemic attack: a statement for healthcare professionals from the American Heart Association/American Stroke Association Council on Stroke: co-sponsored by the Council on Cardiovascular Radiology and Intervention: the American Academy of Neurology affirms the value of this guideline. Stroke. 2006;37(2):577-617.

26. Pandyra A, Mullen PJ, Kalkat M, et al. Immediate utility of two approved agents to target both the metabolic mevalonate pathway and its restorative feedback loop. Cancer Res. 2014;74(17):4772-4782.

27. Ianevski A, Giri AK, Aittokallio T. SynergyFinder 3.0: an interactive analysis and consensus interpretation of multi-drug synergies across multiple samples. Nucleic Acids Res. 2022;50(W1):W739-W743.

28. Gaidano V, Houshmand M, Vitale N, et al. The Synergism between DHODH Inhibitors and Dipyridamole Leads to Metabolic Lethality in Acute Myeloid Leukemia. Cancers (Basel). 2021;13(5):1003.

29. Löffler M, Jöckel J, Schuster G, Becker C. Dihydroorotat-ubiquinone oxidoreductase links mitochondria in the biosynthesis of pyrimidine nucleotides. Mol Cell Biochem. 1997;174(1-2):125-129.

30. Mishra SK, Millman SE, Zhang L. Metabolism in acute myeloid leukemia: mechanistic insights and therapeutic targets. Blood. 2023;141(10):1119-1135.

31. Pereira-Martins DA, Weinhäuser I, Griessinger E, et al. High mtDNA content identifies oxidative phosphorylation-driven acute myeloid leukemias and represents a therapeutic vulnerability. Signal Transduct Target Ther. 2025;10(1):222.

32. Baccelli I, Gareau Y, Lehnertz B, et al. Mubritinib Targets the Electron Transport Chain Complex I and Reveals the Landscape of OXPHOS Dependency in Acute Myeloid Leukemia. Cancer Cell. 2019;36(1):84-99.e8.

33. Jones CL, Stevens BM, D'Alessandro A, et al. Cysteine depletion targets leukemia stem cells through inhibition of electron transport complex II. Blood. 2019;134(4):389-394.

34. Jones CL, Stevens BM, D'Alessandro A, et al. Inhibition of Amino Acid Metabolism Selectively Targets Human Leukemia Stem Cells. Cancer Cell. 2018;34(5):724-740.e4.

35. Teng D, Swanson KD, Wang R, et al. DHODH modulates immune evasion of cancer cells via CDP-Choline dependent regulation of phospholipid metabolism and ferroptosis. Nat Commun. 2025;16(1):3867.

36. Branstrom A, Cao L, Furia B, et al. Emvododstat, a Potent Dihydroorotate Dehydrogenase Inhibitor, Is Effective in Preclinical Models of Acute Myeloid Leukemia. Front Oncol. 2022;12:832816.

Figure legends

Figure 1. Sensitivity to DHODH inhibition of primary AML samples co-cultured on MS5

A. Schematic visualization of the DHODH inhibitor drug screen in primary AML patient samples co-cultured on MS5 cells for seven days. B. Area under the curve (AUC) values, which were calculated using the trapezoid method, and normalized MFI values of CD11b from DHODH treated primary AML cells (n=26) with various mutations co-cultured on MS5 cells. C. Dose-dependent effects on cell viability upon DHODHi treatment of AML16, AML21, AML17 and AML19 under MS5 culture conditions. D. Fold change of viable cell counts of primary AML samples and healthy $CD34^+$ cells of normal bone marrow (NBM) treated with DHODHi both co-cultured on MS5 cells. Statistical analysis by unpaired Student's t test. * $P > 0.05$, ** $P > 0.01$, *** $P > 0.001$, **** $P > 0.0001$.

Figure 2. Integrating drug screening data with quantitative proteome data links DHODHi sensitivity to cholesterol and lipid metabolism

A. Volcano plot of the Pearson correlation coefficient and $-\log_{10}$ p-values of the proteome dataset versus AUC values of DHODHi-treated primary AML samples. B. Dotplot of gene set enrichment analysis (GSEA) signatures enriched in sensitive and less sensitive primary AML patient samples. C. Highlighted gene set enrichment signatures from panel B.

Figure 3. DHODHi increases intracellular cholesterol, ROS and lipid ROS levels while TMRE is reduced

A. MFI fold change of cholesterol (BODIPY-cholesterol) in four-day DMSO or DHODHi-treated (3 nM) HL60 and THP1 cells (n=4 independent experiments). B. MFI fold change of cytoplasmic ROS (DCFDA), mitochondrial superoxide levels (MitoSox), lipid ROS (BODIPY-C11), mitochondrial activity (TMRE) and total mitochondria (Mitotracker green) in four-day DMSO or DHODHi-treated (3 nM) HL60 and THP1 cells. C. Baseline cytoplasmatic ROS, mitochondrial ROS and lipid ROS in HL60 and THP1 cells. Data is normalized to HL60 values. Bar graphs represent the mean ± SEM of at least three independent experiments. Statistical analysis by unpaired Student's t test. * P > 0.05, ** P > 0.01, *** P > 0.001, **** P > 0.0001.

Figure 4. LC-MS/MS-based lipidomics on DHODHi-treated HL60 cells reveals a profound impact on lipid metabolism

A. Volcanoplot showing the differentially expressed lipids of HL60 cells treated with 3 nM of DHODHi versus DMSO for 24 hours. Classes are depicted by colors in the legend. B. Enrichment analysis for lipid classes comparing DHODHi versus DMSO treated cells. C. Total number and relative saturation levels of up and down regulated differentially expressed lipids in DHODHi-treated cells. D. Triglycerides (TGs) abundances in DMSO and DHODHi-treated HL60 cells divided by saturation class. E. MFI fold change of neutral lipids (BODIPY 493/503) in DMSO and DHODHi-treated HL60 cells. Statistical analysis by paired Student's t test (D) and unpaired Student's t test * P > 0.05 (E).

Figure 5. Combination treatment with DHODHi and dipyridamole results in strong synergism in AML cell lines and primary AML samples

A. Impact on relative growth of HL60 and THP1 cells treated for three days with DMSO, DHODHi (0.3, 3.0 and 30 nM) and/or dipyridamole (1, 5 and 10 µM). Representative of three independent experiments. B. Synergy distribution plots of data shown in panel A. C. MFI fold change in cholesterol (BODIPY-cholesterol) in four-day DMSO or 5 µM dipyridamole-treated HL60 and THP1 cells (n=4 independent experiments). Data is normalized to HL60 DMSO values. D. mRNA expression of DHCR7 and HMGCS1 in HL60 and THP1 cells. Data is normalized to HL60 values. Representative of three independent experiments. E. mRNA expression of DHCR7 and HMGCS1 in HL60 and THP1 cells treated with DMSO or 5 µM dipyridamole for 6 and 96 hours, respectively. Data is normalized to DMSO. Representative of three independent experiments. F. Annexin V percentage, CD11b expression and CD14 expression of HL60 and THP1 cells treated with DMSO, DHODHi and dipyridamole for three days. Representatives of three independent experiments. Synergy scores were calculated using the Zero interaction potency (ZIP) model. Bar graphs represent the mean ± SEM of at least three independent experiments. Statistical analysis by unpaired Student's t test. * $P > 0.05$, ** $P > 0.01$, *** $P > 0.001$, **** $P > 0.0001$.

Figure 1

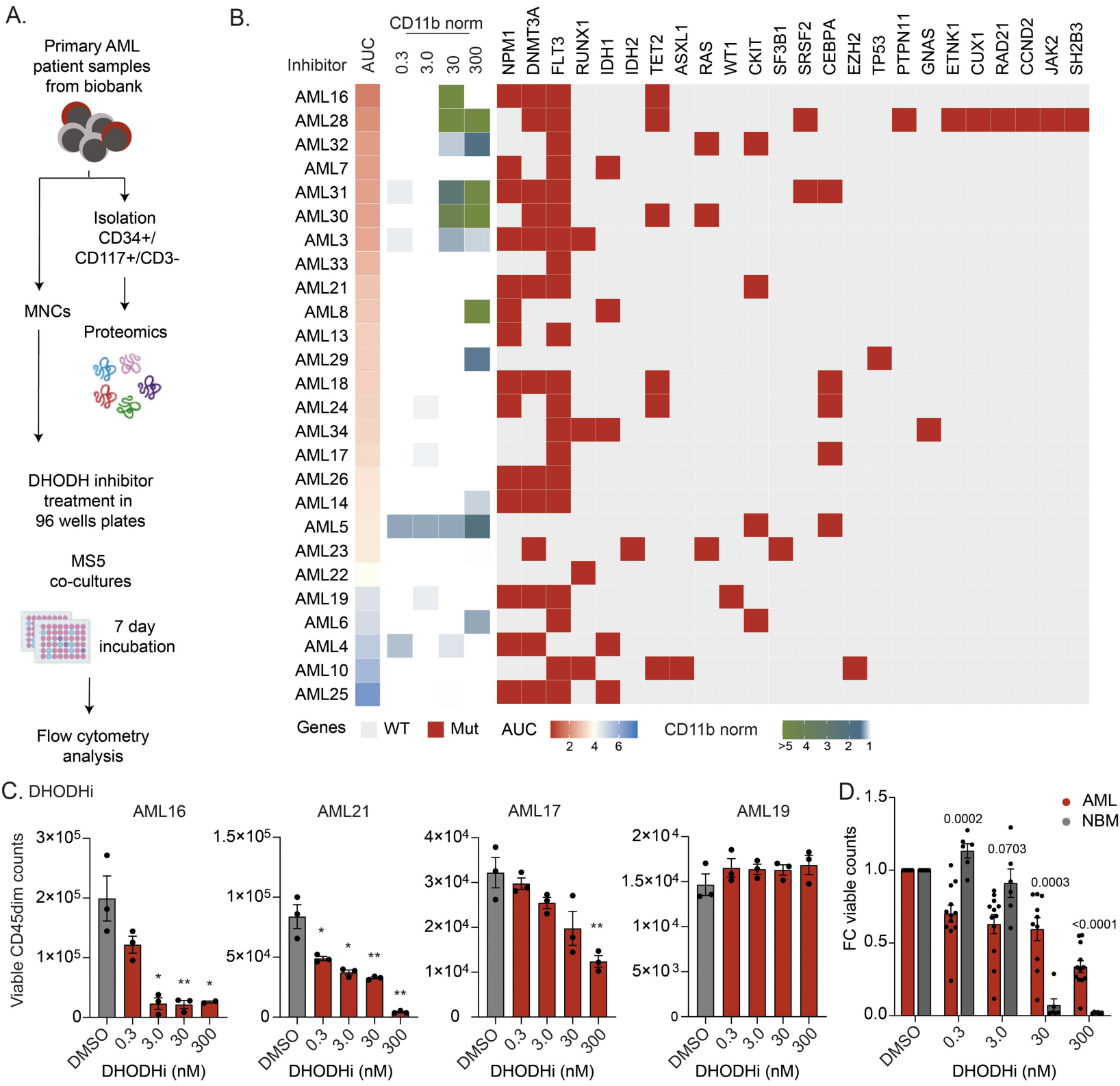
A.
Primary AML patient samples from biobank
Isolation CD34+/ CD117+/CD3-
MNCs
Proteomics
DHODH inhibitor treatment in 96 wells plates
MS5 co-cultures
7 day incubation
Flow cytometry analysis
B.
Inhibitor
AUC
CD11b norm
0.3
3.0
30
300
NPM1
DNMT3A
FLT3
RUNX1
IDH1
IDH2
TET2
ASXL1
RAS
WT1
CKIT
SF3B1
SRSF2
CEBPA
EZH2
TP53
PTPN11
GNAS
ETNK1
CUX1
RAD21
CCND2
JAK2
SH2B3
AML16
AML28
AML32
AML7
AML31
AML30
AML3
AML33
AML21
AML8
AML13
AML29
AML18
AML24
AML34
AML17
AML26
AML14
AML5
AML23
AML22
AML19
AML6
AML4
AML10
AML25
Genes
WT
Mut
AUC
2 4 6
CD11b norm
>5 4 3 2 1
C. DHODHi
AML16
AML21
AML17
AML19
Viable CD45dim counts
DHODHi (nM)
DMSO
0.3
3.0
30
300
D.
AML
NBM
FC viable counts
0.0002
0.0703
0.0003
<0.0001
DHODHi (nM)

Figure 2

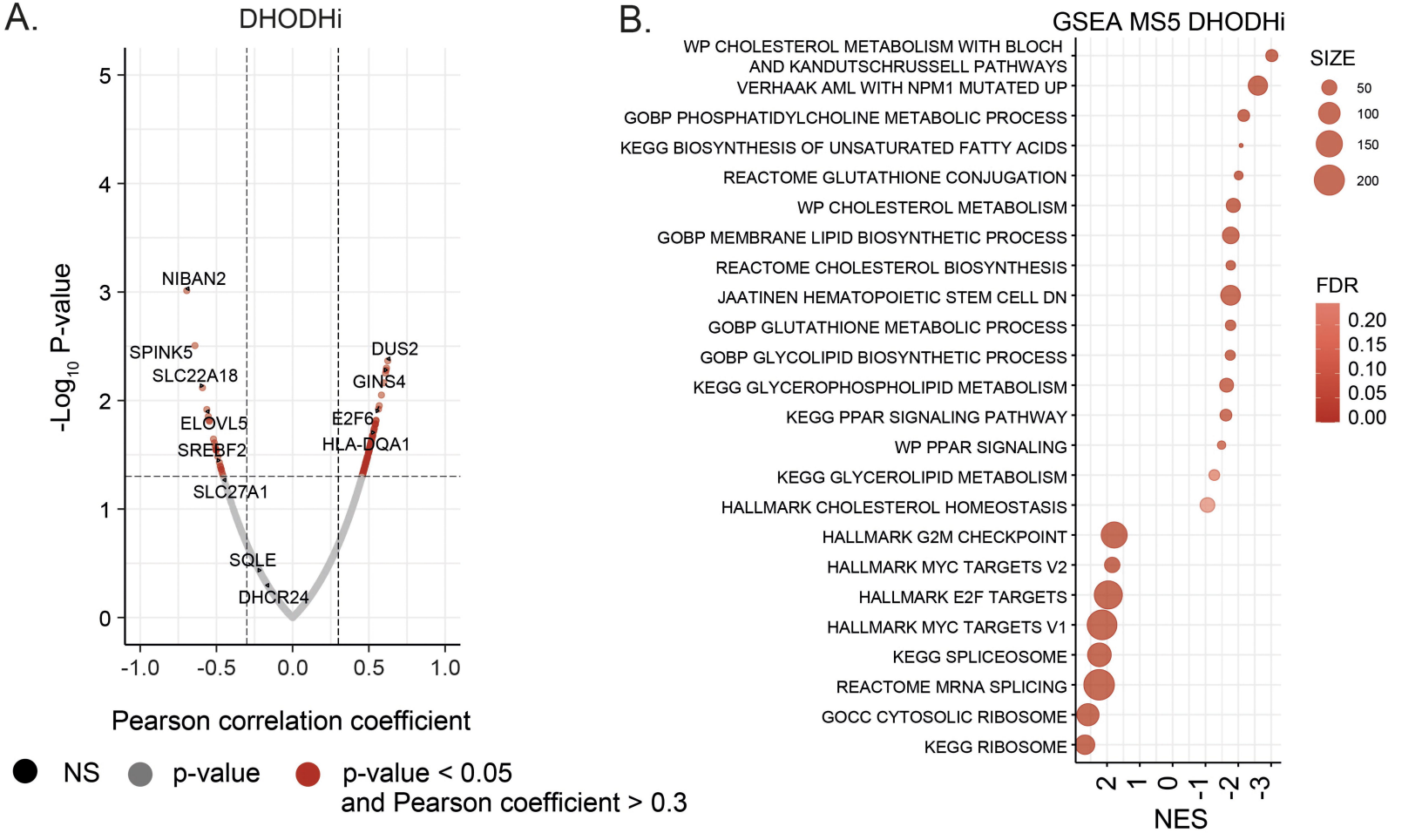
A.
DHODHi
-Log10 P-value
Pearson correlation coefficient
NIBAN2
SPINK5
SLC22A18
ELOVL5
SREBF2
SLC27A1
SQLE
DHCR24
DUS2
GINS4
E2F6
HLA-DQA1
NS
p-value
p-value < 0.05
and Pearson coefficient > 0.3
B.
GSEA MS5 DHODHi
WP CHOLESTEROL METABOLISM WITH BLOCH AND KANDUTSCHRUSSELL PATHWAYS
VERHAAK AML WITH NPM1 MUTATED UP
GOBP PHOSPHATIDYLCHOLINE METABOLIC PROCESS
KEGG BIOSYNTHESIS OF UNSATURATED FATTY ACIDS
REACTOME GLUTATHIONE CONJUGATION
WP CHOLESTEROL METABOLISM
GOBP MEMBRANE LIPID BIOSYNTHETIC PROCESS
REACTOME CHOLESTEROL BIOSYNTHESIS
JAATINEN HEMATOPOIETIC STEM CELL DN
GOBP GLUTATHIONE METABOLIC PROCESS
GOBP GLYCOLIPID BIOSYNTHETIC PROCESS
KEGG GLYCEROPHOSPHOLIPID METABOLISM
KEGG PPAR SIGNALING PATHWAY
WP PPAR SIGNALING
KEGG GLYCEROLIPID METABOLISM
HALLMARK CHOLESTEROL HOMEOSTASIS
HALLMARK G2M CHECKPOINT
HALLMARK MYC TARGETS V2
HALLMARK E2F TARGETS
HALLMARK MYC TARGETS V1
KEGG SPLICEOSOME
REACTOME MRNA SPLICING
GOCC CYTOSOLIC RIBOSOME
KEGG RIBOSOME
NES
SIZE
FDR

C.

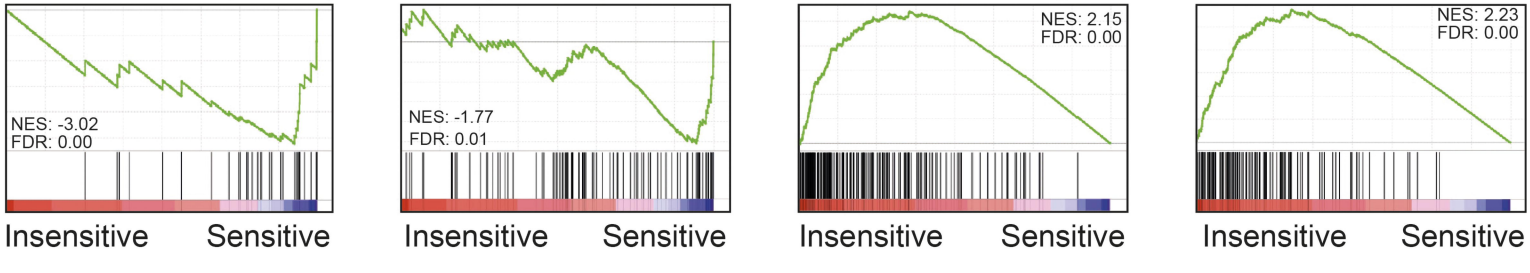
WP Cholesterol metabolism with bloch and kandutschrussell pathways
NES: -3.02
FDR: 0.00
GOBP Membrane lipid biosynthetic process
NES: -1.77
FDR: 0.01
HALLMARK MYC targets v1
NES: 2.15
FDR: 0.00
KEGG Spliceosome
NES: 2.23
FDR: 0.00
Insensitive
Sensitive

Figure 3

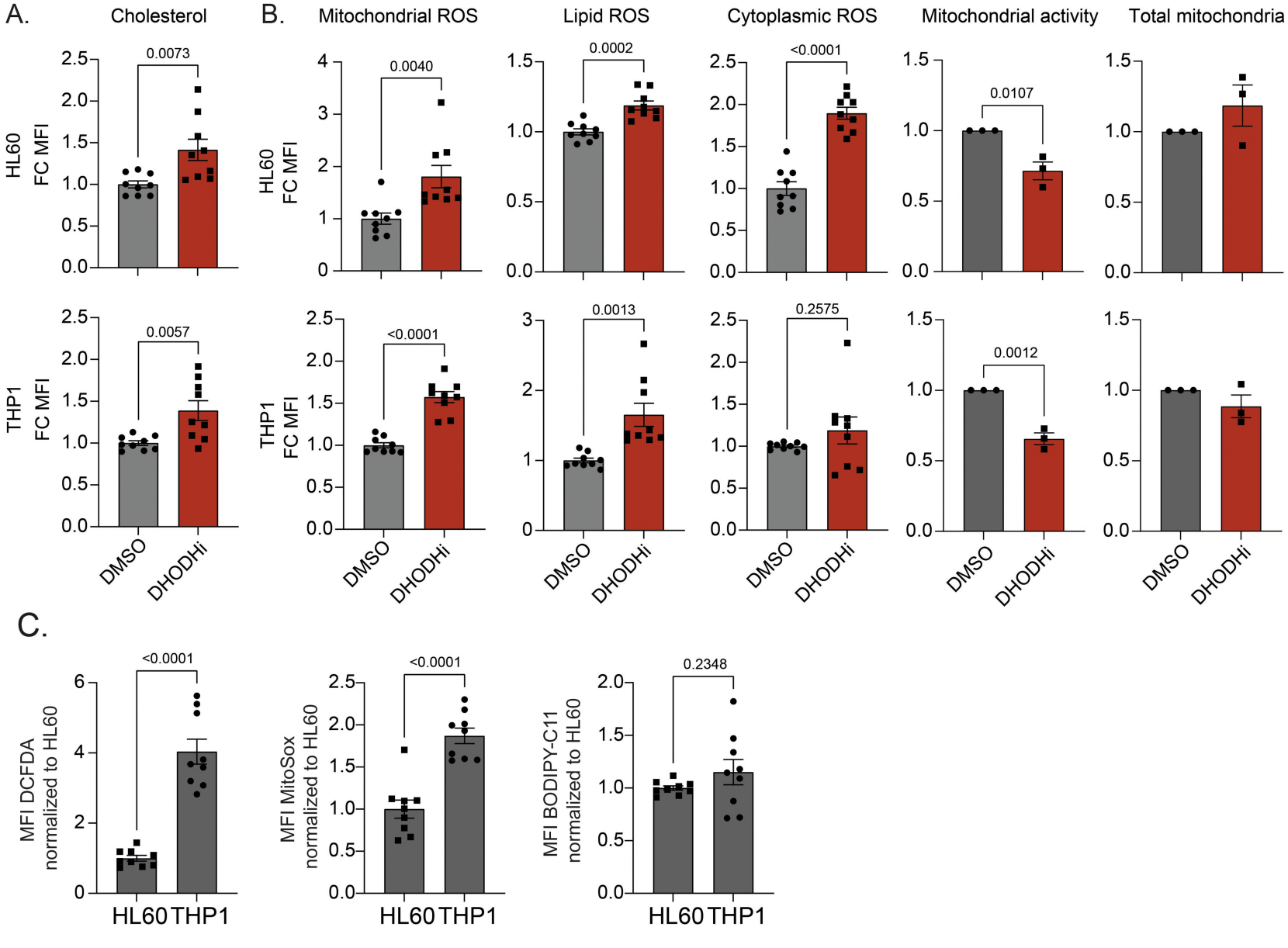
A.
Cholesterol
HL60 FC MFI
THP1 FC MFI
0.0073
0.0057
B.
Mitochondrial ROS
Lipid ROS
Cytoplasmic ROS
Mitochondrial activity
Total mitochondria
0.0040
0.0002
<0.0001
0.0107
<0.0001
0.0013
0.2575
0.0012
DMSO
DHODHi
C.
MFI DCFDA normalized to HL60
MFI MitoSox normalized to HL60
MFI BODIPY-C11 normalized to HL60
<0.0001
<0.0001
0.2348
HL60 THP1

Figure 4

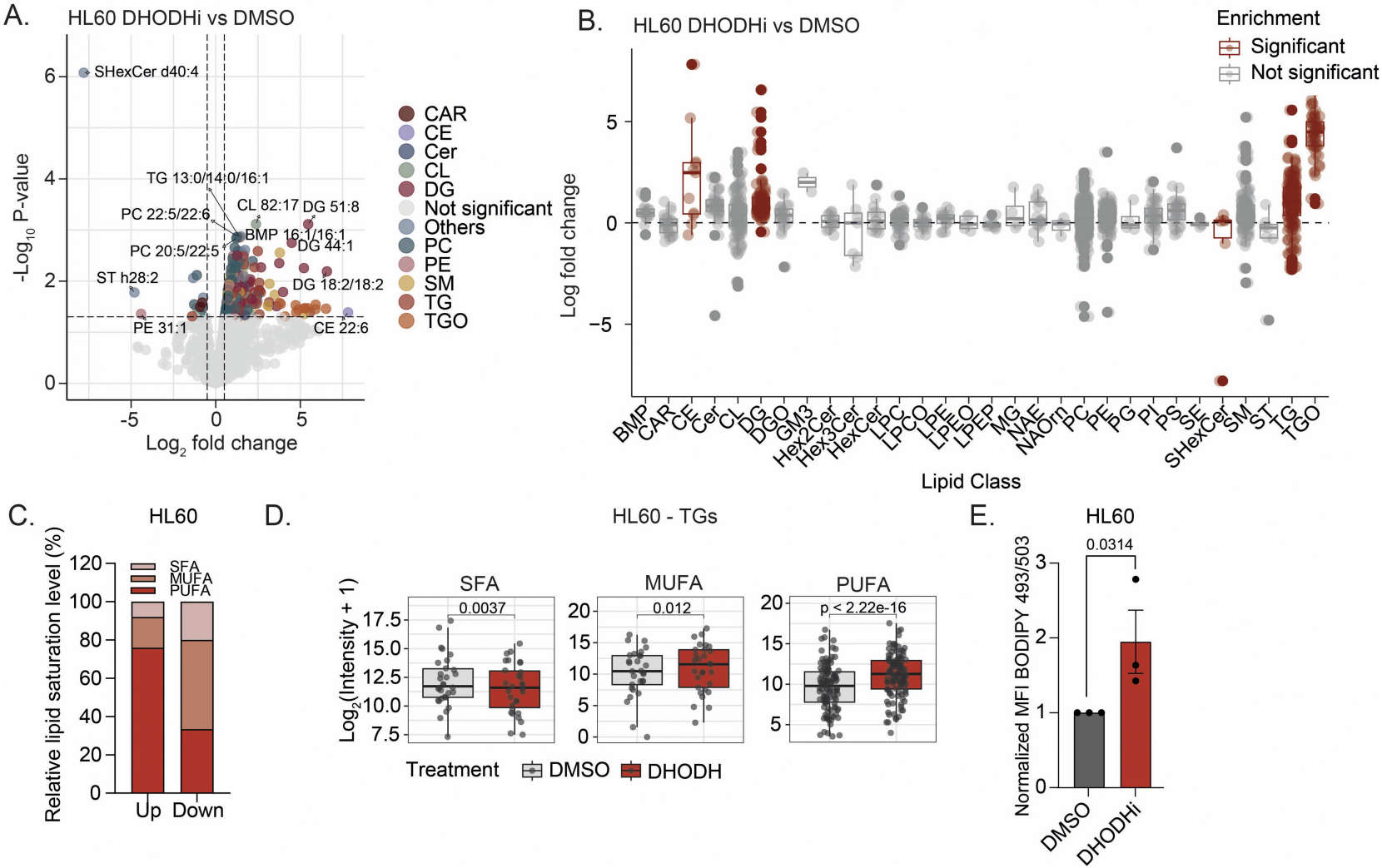
A.
HL60 DHODHi vs DMSO
SHexCer d40:4
TG 13:0/14:0/16:1
PC 22:5/22:6
CL 82:17
DG 51:8
BMP 16:1/16:1
PC 20:5/22:5
DG 44:1
ST h28:2
DG 18:2/18:2
PE 31:1
CE 22:6
-Log10 P-value
Log2 fold change
CAR
CE
Cer
CL
DG
Not significant
Others
PC
PE
SM
TG
TGO
B.
HL60 DHODHi vs DMSO
Enrichment
Significant
Not significant
Log fold change
BMP CAR CE Cer CL DG DGO GM3 Hex2Cer Hex3Cer HexCer LPC LPCO LPE LPEO LPEP MG NAE NAOrn PC PE PG PI PS SE SHexCer SM ST TG TGO
Lipid Class
C.
HL60
Relative lipid saturation level (%)
SFA
MUFA
PUFA
Up
Down
D.
HL60 - TGs
SFA
MUFA
PUFA
0.0037
0.012
p < 2.22e-16
Log2(Intensity + 1)
Treatment
DMSO
DHODH
E.
HL60
0.0314
Normalized MFI BODIPY 493/503
DMSO
DHODHi

Figure 5

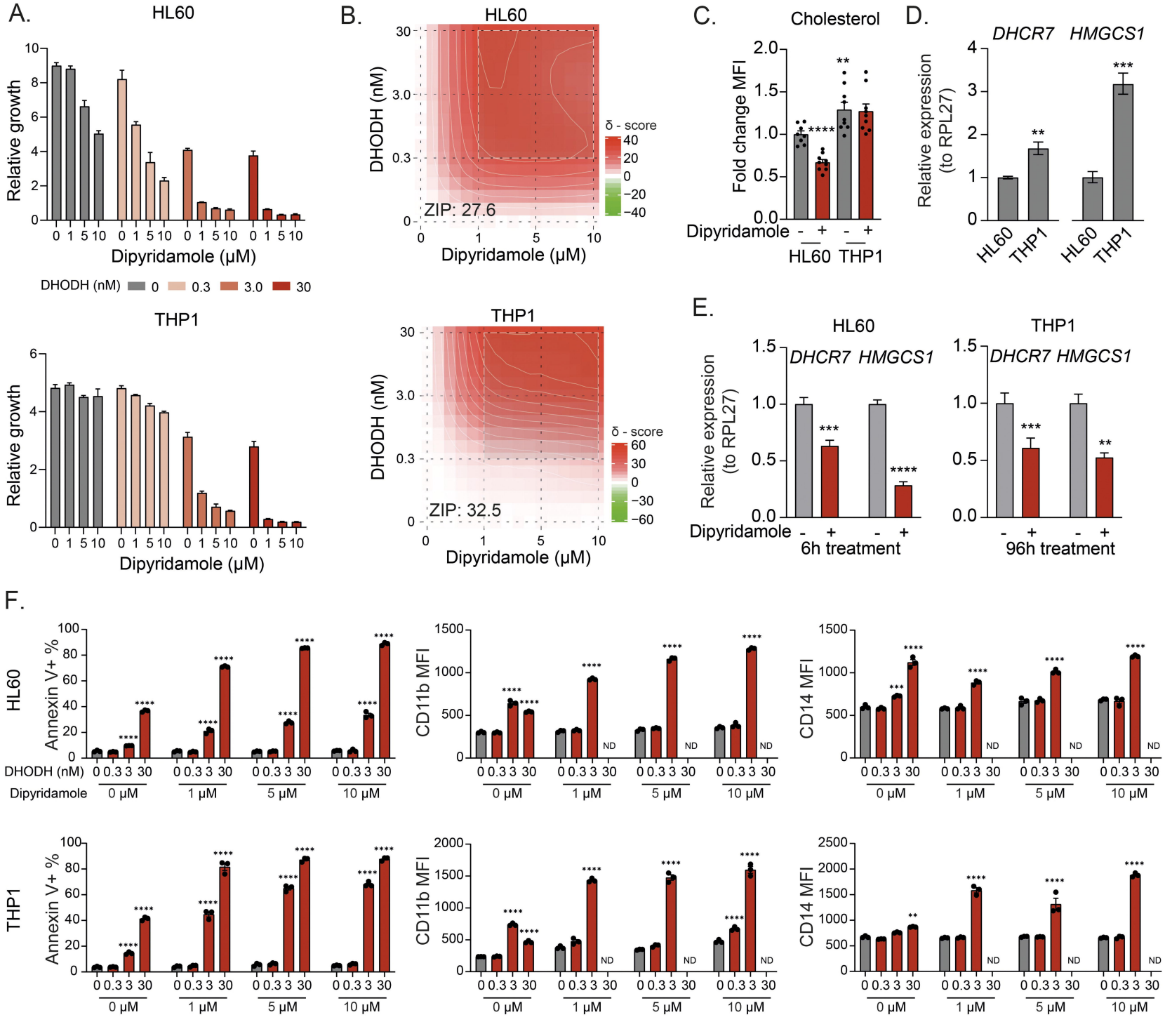
A.
HL60
Relative growth
Dipyridamole (μM)
DHODH (nM) 0 0.3 3.0 30
THP1
B.
HL60
DHODH (nM)
Dipyridamole (μM)
δ - score
ZIP: 27.6
THP1
ZIP: 32.5
C.
Cholesterol
Fold change MFI
Dipyridamole
HL60 THP1
D.
DHCR7 HMGCS1
Relative expression (to RPL27)
HL60 THP1
E.
HL60
THP1
DHCR7 HMGCS1
Relative expression (to RPL27)
Dipyridamole
6h treatment
96h treatment
F.
HL60
THP1
Annexin V+ %
CD11b MFI
CD14 MFI
DHODH (nM) 0 0.3 3 30
Dipyridamole 0 μM 1 μM 5 μM 10 μM
ND

Supplementary Materials and Methods and Supplementary Figures

Potent synergy of DHODH and SREBP inhibition in acute myeloid leukemia via disruption of cholesterol and lipid metabolism

Shanna M. Hogeling[1], Dominique Sternadt[1], Nikita La Rose[1], Diego Pereira-Martins[1], Marjan Geugien[1], Fiona A.J. van den Heuvel[1], Anna Kuchnio[2], E. Christine Pietsch[3], Ulrike Philippar[2], Gerwin Huls[1] and Jan Jacob Schuringa[1*]

[1]Department of Hematology, University Medical Center Groningen, University of Groningen, Groningen, The Netherlands

[2]Discovery Oncology, Janssen Research & Development, Beerse, BE

[3]Discovery Oncology, Janssen Research & Development, Spring House, US

[*]correspondence:

Prof.dr. J.J. Schuringa, PhD

Department of Experimental Hematology

University Medical Center Groningen

Hanzeplein 1, PO Box 30.001, 9700 RB Groningen, The Netherlands

Phone: + 31503612354, Fax: +31503615960

E-mail: j.j.schuringa@umcg.nl

Supplementary Materials and Methods

Quantitative real-time PCR

RNA samples were prepared from cell lines and primary AML patient samples treated with DMSO or menin inhibitor for various timepoints. Total RNA was isolated using the RNeasy Mini Kit from Qiagen (Venlo, The Netherlands) according to the manufacturer's protocol and reverse transcribed using the iScript cDNA synthesis kit (Bio-Rad). Subsequently, the cDNA was amplified using SsoAdvanced SYBR Green Supermix (Bio-Rad) on a CFX384 Touch Real-Time PCR Detection System (Bio-Rad). Primer sequences are listed in table 1.

Table 1. Primers used for mRNA expression

Target	Forward	Reverse
DHCR7	AGGACTTTAGCCGGTTGAGA	AGCCATTGGGCCCTCC
HMGCS1	TCTATCCTTCACACAGCTCTTTC	TCTCAAGGGCAACAATTCCC
ACTB	AGGCCAACCGCAAGAAG	ACAGCCTGGATAGCAACGTACA
RPL30	ACTGCCCAGCTTTGAGGAAAT	TGCCACTGTAGTGATGGACAC

LC-MS/MS analysis

Lipids were analyzed with liquid chromatography-tandem mass spectrometry (LC-MS/MS) on a Shimadzu LC40 UPLC system coupled to a ZenoTOF 7600 mass spectrometer (Sciex). 2 µL lipid extracts were injected and separated on a Waters Acquity CSH C18 1.7 um, 2.1 x 100 mm column, with a gradient of mobile phase A consisting of 40/60/0.1 water/acetonitrile/formic acid + 10 mM ammonium formate and mobile phase B consisting of 10/89/1/0.1 acetonitrile/isopropanol/water/formic acid + 10 mM ammonium formate. The concentration of B was increased from 20 to 50% in 2.1 min, and the to 54% in 9.8 min. It was then increased to 70% in 0.1 min and to 99% in 5.9 min and decreased to 20% in 0.1 min where it was held for 1.9 min. The total run time was 20 min, the flow rate was 0.4 mL/min and the column temperature 55 °C. MS data acquisition was performed in positive mode using data dependent acquisition at a declustering potential of 50 V. An 100 ms MS1 survey scan at m/z 100-2000 was

followed by up to 40 data dependent MS2 scans (Top40), of precursor ions exceeding 100 cps. MS2 scans using collision induced dissociation (CID) were acquired at m/z 50-2000 using Zeno trapping, for 5 ms and at a collision energy of 40 eV, with a Zeno threshold of 20000 cps.

Untargeted data analysis with MS-DIAL

Data analysis was performed with MS-DIAL version 5.5.250404 using the lipidomics workflow: 24 data files were processed and aligned, and normalized with SPLASH using peak intensities. Reference-matched lipids were exported as a csv file for further data analysis. For further data analysis, data was log-2 transformed before using the package lipidr[1] to perform differential and enrichment analysis of lipid classes, carbon lengths and unsaturation levels.

LFQ proteome data analysis

The LFQ proteome dataset on primary AML samples that were thawed and sorted for CD34+ or CD117+ was previously published (PXD030487).[7] Pearson correlations with the PFQ proteome were performed using the calculated AUC and only genes with a row max of > 50 were taken along in further analysis. Gene set enrichment analysis were performed using ranked pearson coefficient values.

Statistics

All statistical analyses were performed using the student t test paired or unpaired and were expressed as means ± SEM for all other comparisons. Differences were considered statistically significant at $p \leq 0.05$.

References

1. Mohamed A, Molendijk J, Hill MM. Lipidr: A Software Tool for Data Mining and Analysis of Lipidomics Datasets. J Proteome Res 2020;19(7):2890–2897.

Supplementary Tables – See Excel files

Supplementary table 1. Overview of patient samples included in study. Viability data associated with Supplementary Figure 1C, area under the curve (AUC) and CD11b data associated with Figure 1B, ZIP scores associated with Supplementary Figure 4E and mutation status are shown.

Supplementary table 2. Lipidomics data. LC-MS/MS based lipidome data of HL60 and THP1 cells treated with DHODHi for 24h.

Supplementary Figures

Supplementary Figure 1. Sensitivity to DHODH inhibition of primary AML samples co-cultured on MS5

A. Schematic overview depicting the gating strategy used in the DHODHi drug screen. B-C. Viability of primary AML samples co-cultured for seven days on MS5. D. Comparison of AUC values from primary AML patient samples treated with the DHODH inhibitor versus the proliferation index (PI). E. Boxplots showing DHODHi AUC values of the proliferation of mutant vs wild type subgroups. F-G. Dose-dependent effect on proliferation, normalized Annexin V (%), normalized CD11b MFI and normalized CD14 MFI in cell lines HL60 and THP1 upon treatment with DHODHi (n=6 independent experiments). Statistical analysis by unpaired Student's t test (E), one-way ANOVA (F-G) or Simple Linear Regression (D).

Supplementary Figure 2. ssGSEA analysis of DHODHi-sensitive primary AML samples shows a diverse metabolic program.

Single sample GSEA (ssGSEA) of eight DHODHi-sensitive primary AML samples showing a selection of metabolism signatures. Area under the curve (AUC) values are taken from the drug screen data in figure 1B.

Supplementary Figure 3. LC-MS/MS-based lipidomics on DHODHi-treated THP1 cells reveals a profound impact on lipid metabolism

A. Volcanoplot showing the differentially expressed lipids of THP1 cells treated with 3 nM of DHODHi versus DMSO for 24 hours. Classes are depicted by colors in the legend. B. Enrichment analysis for lipid classes comparing DHODHi versus DMSO treated cells. C. Volcanoplot showing differentially expressed lipids of HL60 cells versus THP1 cells. D. Enrichment analysis for lipid classes comparing HL60 versus THP1 cells. E. Total number and relative saturation levels of up and down regulated differentially expressed lipids in DHODHi-treated cells. F. Triglycerides (TGs) abundances in DMSO and DHODHi-treated THP1 cells divided by saturation class. G. MFI fold change of neutral lipids (BODIPY 493/503) in DMSO and DHODHi-treated THP1 cells. Statistical analysis by paired Student's t test (F) and unpaired Student's t test * $P > 0.05$ (G).

Supplementary Figure 4. Combination treatment with DHODHi and dipyridamole results in strong synergism in AML cell lines and primary AML samples

A. Dose-dependent effect on proliferation in THP1 cells upon treatment with dipyridamole cultured in RPMI with FCS and P/S. Representative of three independent experiments. B. MFI fold change in cholesterol (BODIPY-cholesterol) in four-day dose-

dependent dipyridamole-treated THP1 cells. Bar graphs represent the mean ± SEM of at least three independent experiments. C. Log2 expression of transcriptome data obtained from CCLE of cell lines HL60 and THP1. D. Treatment of AML3, AML6, AML14 and AML27 with DMSO, DHODHi (0.3, 3.0 and 30 nM) and dipyridamole (1, 5 and 10 μM) for four days co-cultured on MS5 cells. Synergy distribution plots of treated AML patient samples. E. Summary of primary AML samples treated with DHODHi and dipyridamole showing effect on proliferation ($CD45^+/7AAD^-$ viable counts; n=14) and differentiation (MFI of CD11b and CD14; n=10). Per AML values are normalized to the DMSO control. Statistical analysis by unpaired Student's t test or one-way ANOVA. * P > 0.05, ** P > 0.01, *** P > 0.001, **** P > 0.0001.

Supplementary Figure 5. Effects of combined DHODHi and dipyridamole on viable cell counts of normal CD34+ cells compared to primary AML samples

A. Normalized viable cell counts ($CD45^+/7AAD^-$ or $CD34^+/7AAD^-$ (CB)) of primary AML samples (n=14) and healthy $CD34^+$ cord blood (CB) cells (n=4) treated with DHODHi and dipyridamole (5 and 10 μM) both co-cultured on MS5 cells. B-C. Effect on differentiation shown by MFI values of CD11b and CD14 from healthy $CD34^+$ CB treated with DHDOHi and dipyridamole. Statistical analysis by one-way ANOVA. * P > 0.05, ** P > 0.01, *** P > 0.001, **** P > 0.0001.

Supplementary Figure 6. Combination treatment of DHODHi with ENT or cholesterol inhibitors reveal heterogeneous responses

A. HL60 and THP1 cells treated with DHODHi and ENT inhibitor Dilazep (0,1, 1 and 10 μM). Representative of three independent experiments. B. Synergy distribution plots of data shown in panel A and of two primary AML samples treated with DHODHi

and Dilazep. C. HL60 and THP1 cells treated with DHODHi and cholesterol inhibitor Rosuvastatin (0,3, 3 and 30 μM). Representative of three independent experiments. D. Synergy distribution plots of data shown in panel C and of one primary AML sample treated with DHODHi and Rosuvastatin. E. HL60 and THP1 cells treated with DHODHi and cholesterol inhibitor Atorvastatin (2, 10 and 20 μM). Representative of three independent experiments. F. Synergy distribution plots of data shown in panel E. All data is normalized to DMSO controls. Statistical analysis by one-way ANOVA. * P > 0.05, ** P > 0.01, *** P > 0.001, **** P > 0.0001.

Supplementary Figure 1

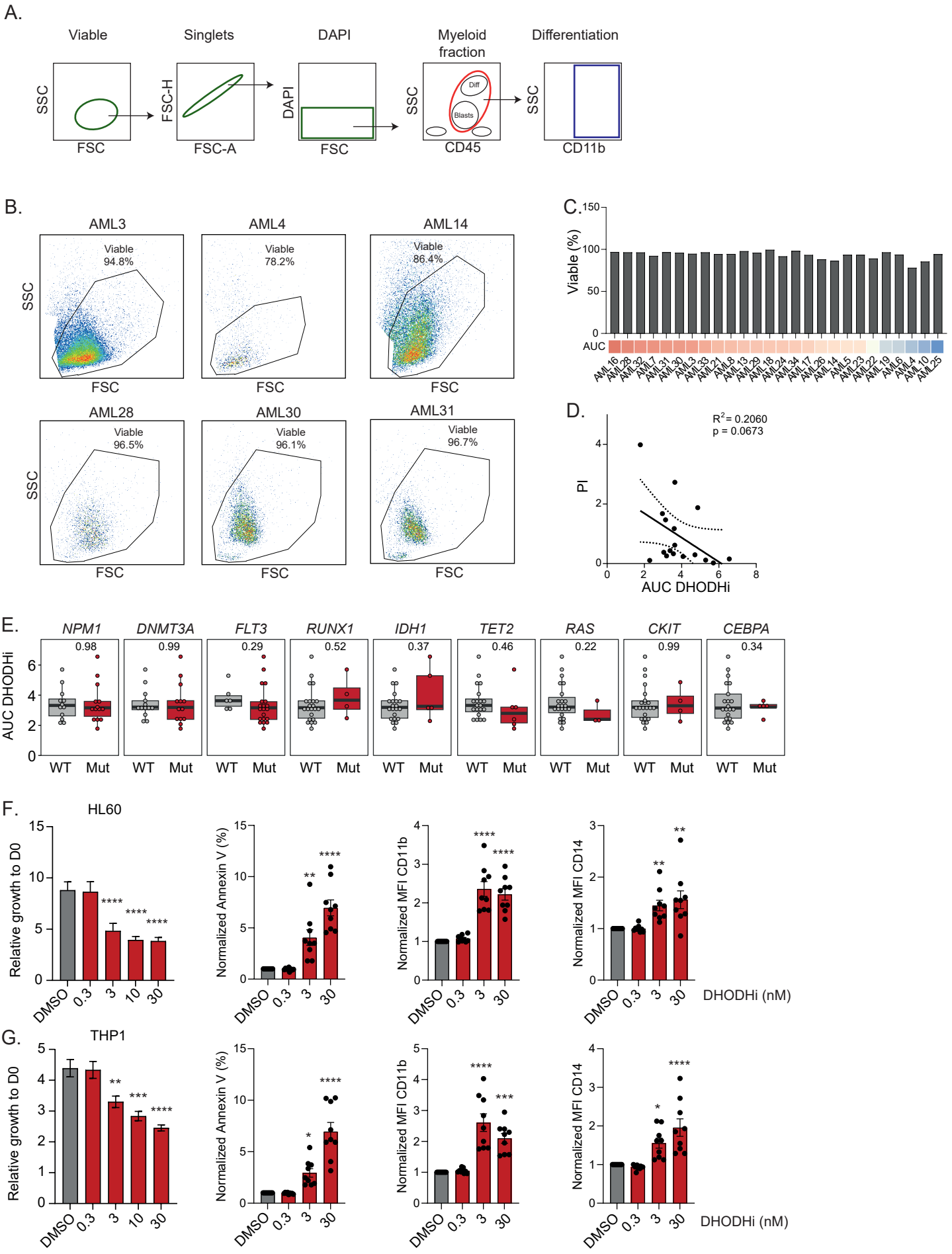

Supplementary Figure 2

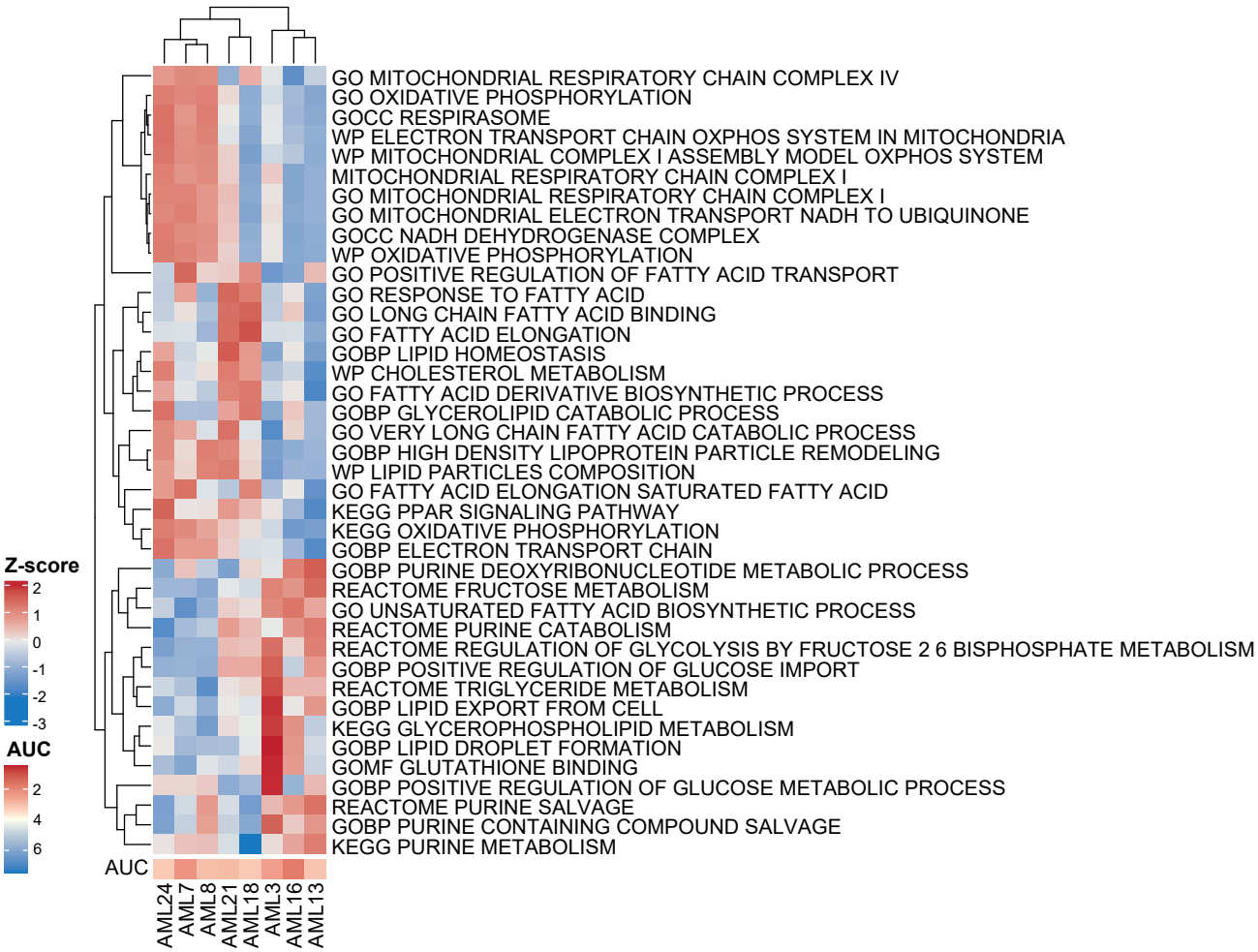

Supplementary Figure 3

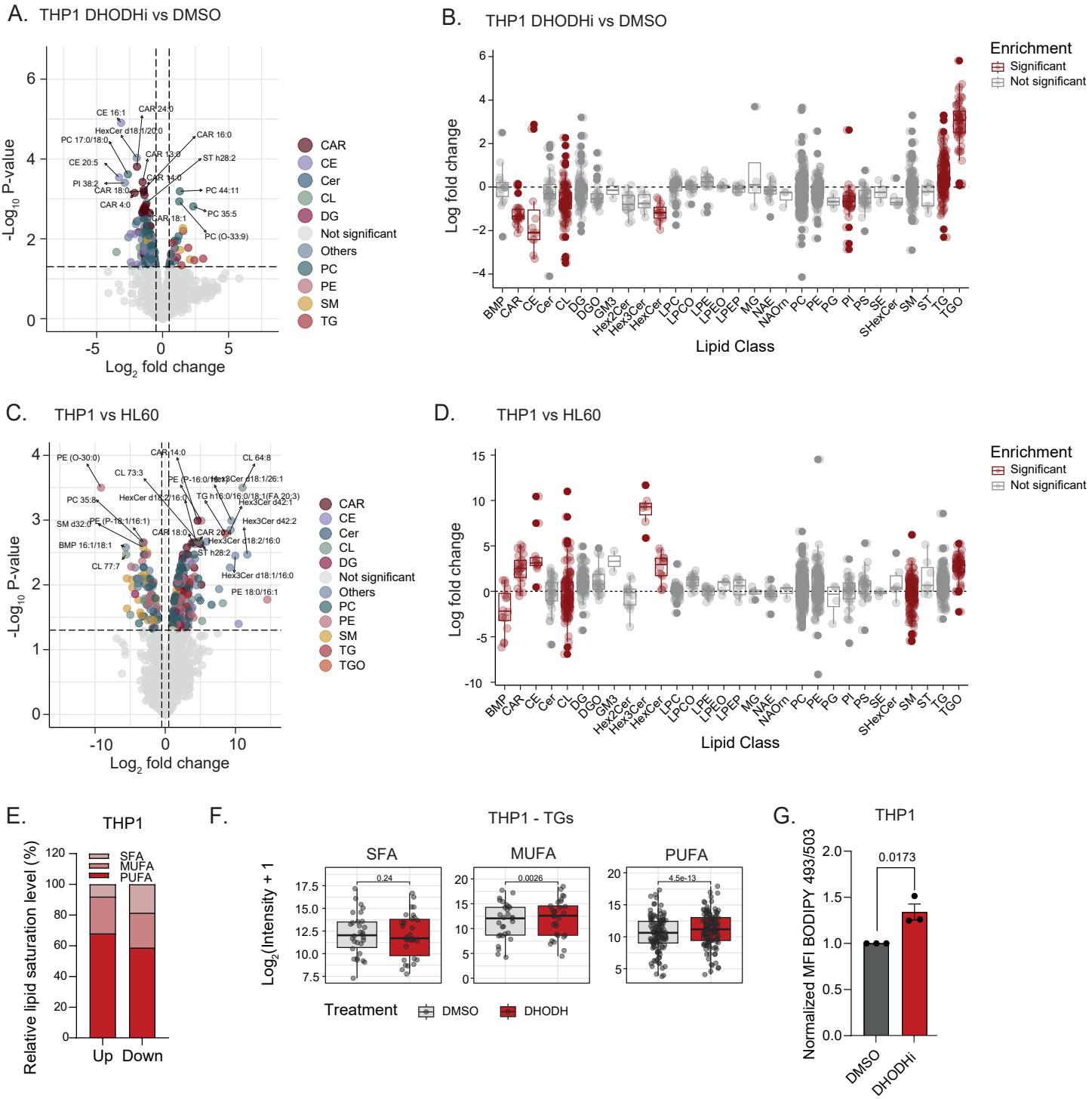

Supplementary Figure 4

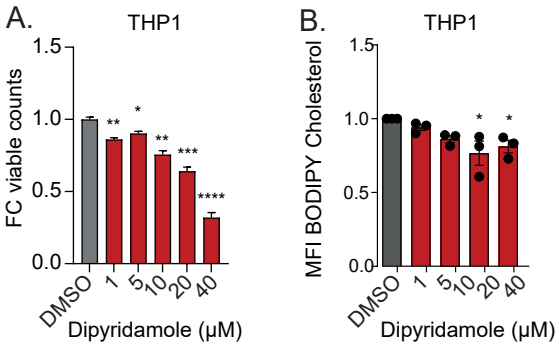

C.

	HL60	THP1
HMGCS1	2.89	5.49
HMGCR1	2.11	5.83
MVK	2.42	3.58
PMVK	4.10	5.58
MVD	3.54	5.75
IDI1	4.09	5.14
FDPS	7.32	8.80
FDFT1	5.90	8.38
SQLE	2.92	6.65
LSS	2.90	4.83
SC5D	2.05	4.80
GGPS1	3.17	5.02
DHCR24	4.80	6.51
DHCR7	3.95	4.54
SLC29A1	6.73	6.80
SLC29A2	4.52	0.82
SLC29A3	1.48	2.06

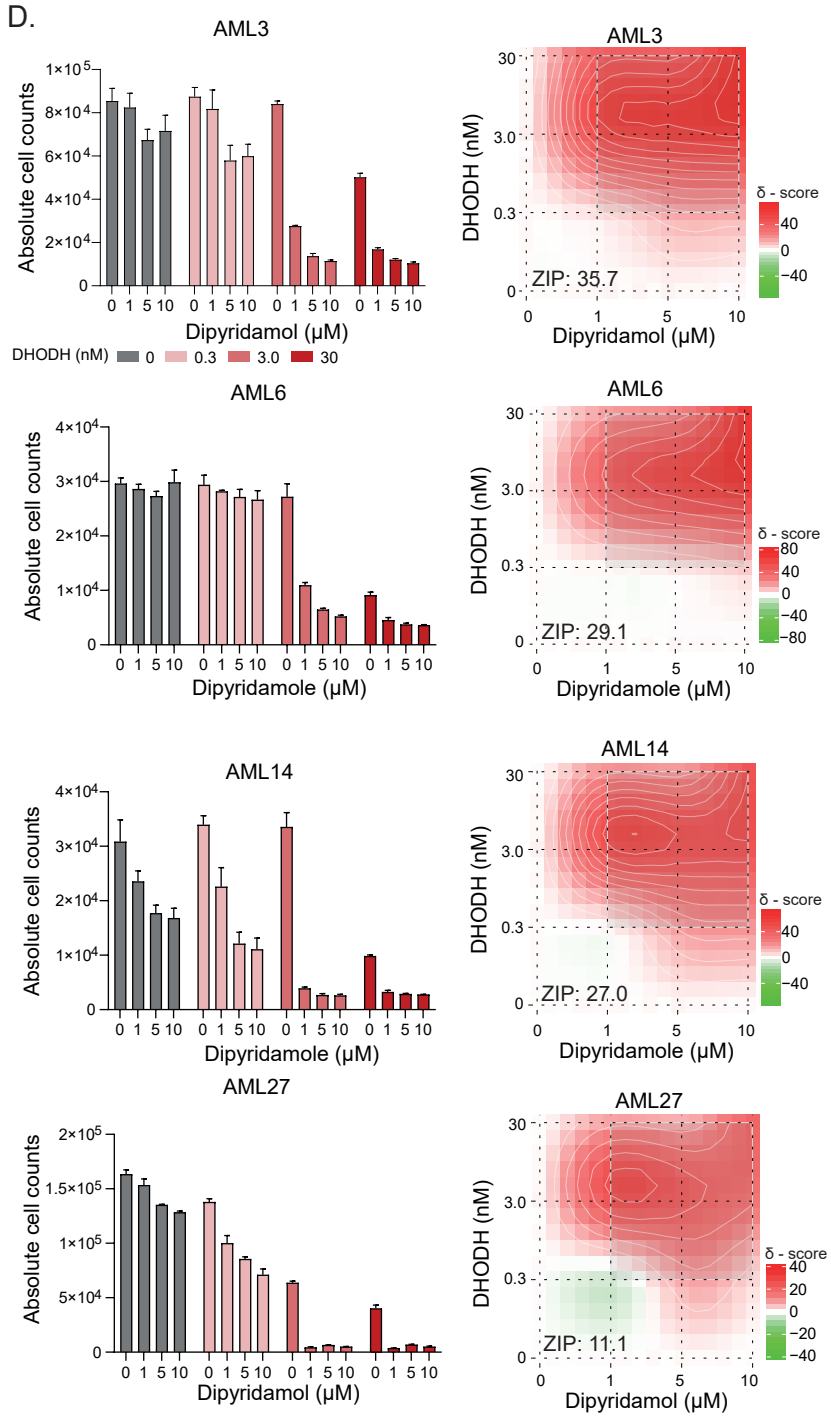

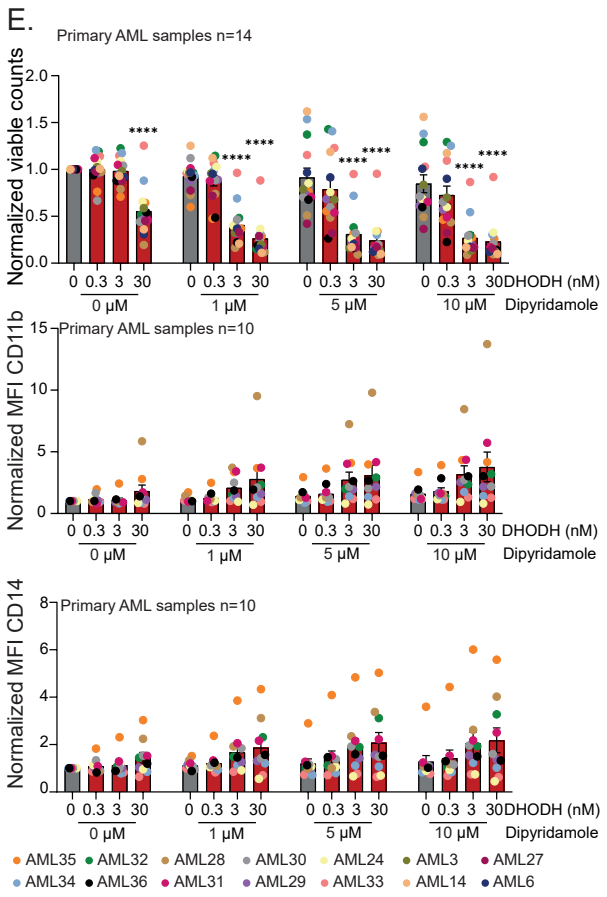

Supplementary Figure 5

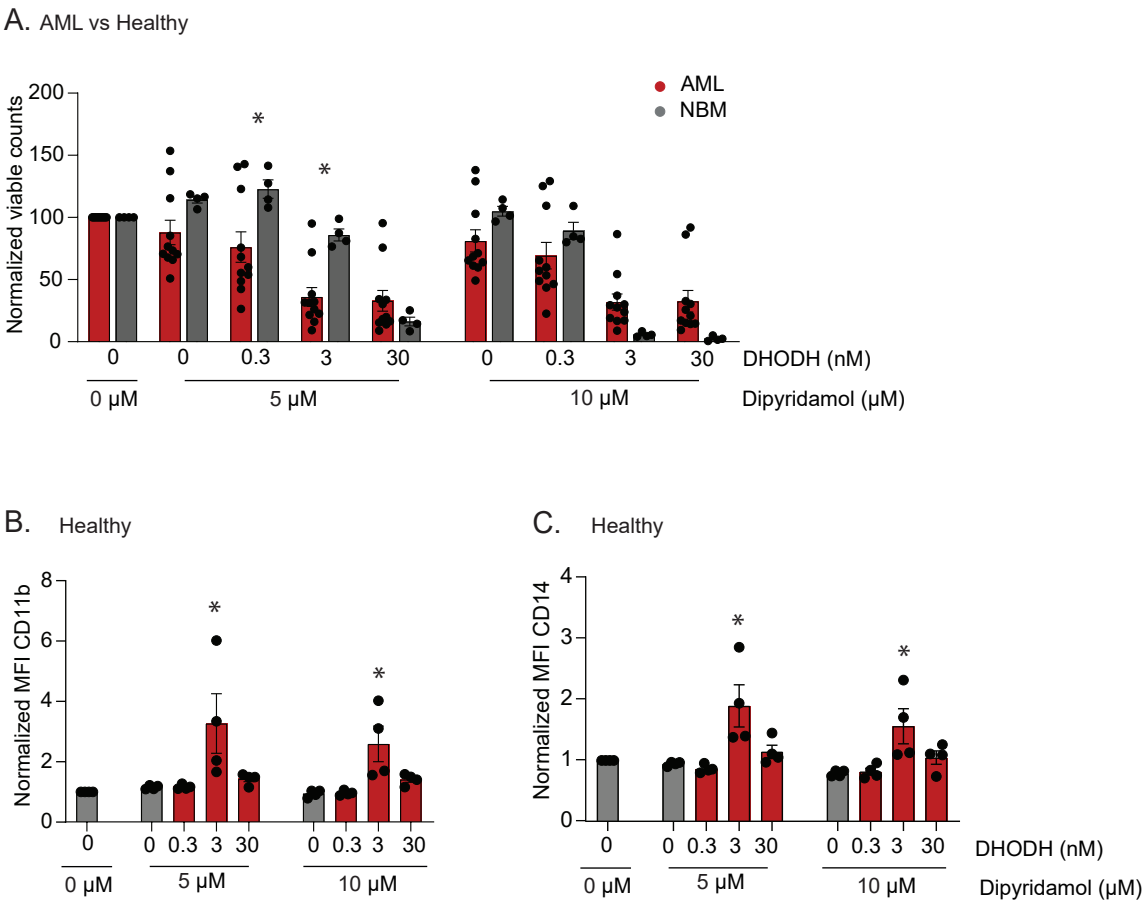

Supplementary Figure 6